Int J Clin Exp Pathol 2016;9(5):5722-5732
www.ijcep.com /ISSN:1936-2625/IJCEP0027993

Case Report

Erionite-associated malignant pleural mesothelioma in Mexico

Elizabeth A Oczypok[1], Matthew S Sanchez[2], Drew R Van Orden[2], Gerald J Berry[3], Kristina Pourtabib[4], Mickey E Gunter[4], Victor L Roggli[5], Alyssa M Kraynie[5], Tim D Oury[1]

[1]Department of Pathology, University of Pittsburgh School of Medicine, Pittsburgh, PA, 15213; [2]RJ Lee Group, Inc., Monroeville, PA, 15146; [3]Department of Pathology, Stanford University School of Medicine, Stanford, CA, 94305; [4]Department of Geological Sciences, University of Idaho, Moscow, ID, 83844; [5]Department of Pathology, Duke University School of Medicine, Durham, NC, 27710

Received March 11, 2016; Accepted March 28, 2016; Epub May 1, 2016; Published May 15, 2016

Abstract: Malignant mesothelioma is a highly fatal cancer of the visceral and parietal pleura most often caused by asbestos exposure. However, studies over the past thirty-five to forty years have shown that a fibrous zeolite mineral found in the soil, erionite, is a strong causative agent of malignant mesothelioma as well. Cases of erionite-associated pleural mesothelioma have been widely reported in Turkey, but only one case has been documented in North America. Here we report a new North American case of epithelial malignant pleural mesothelioma in a vehicle repairman who was raised on a farm in the Mexican Volcanic Belt region. The complexities of the case highlight the importance of objective lung digestion studies to uncover the causative agents of mesotheliomas. It also highlights a need for increased environmental precautions and medical vigilance for mesotheliomas in erionite-rich regions of the United States and Mexico.

Keywords: Mesothelioma, erionite, zeolite, asbestos

Introduction

Mesothelioma is a rare yet aggressive cancer of the mesothelial cells of the serous membranes of the pleural, pericardial, and peritoneal cavities, and less often, the tunica vaginalis testis. Exposure to amphibole asbestos is the most common cause of malignant pleural mesothelioma. Mesotheliomas caused by exposure to asbestos typically have a latency period of about 20-50 years [1]. In addition to asbestos, recent studies have highlighted the role of another cause of mesotheliomas: the fibrous form of the mineral erionite. Erionite is a zeolite mineral found mostly in volcanic regions. Some of the highest concentrations of this fiber can be found in the Intermountain West of the United States, extending from Oregon and into Mexico and the Sierra Madre Occidental region [2, 3].

Early studies in rodents demonstrated that erionite was a potent carcinogen and was 200 times more pathologic than crocidolite asbestos in causing mesotheliomas [4, 5]. Mesothelioma resulting from erionite exposure was first recognized in Turkey, where large clusters of people in the Cappadocia region presented with pleural mesotheliomas [6, 7]. Subsequent studies found that erionite from the soil was the cause of these malignant mesotheliomas in Turkey [8].

Recently, several studies have suggested that there are higher than normal rates of mesothelioma in certain areas of the Intermountain West and Mexico [2, 9-13]. One study has also provided epidemiological evidence for increased rates of mesothelioma in Tierra Blanca de Abajo in San Miguel de Allende, Guanajuato, Mexico [14]. Many of these cases have been among people who have had little to no occupational exposure to asbestos. In 2008, Kliment *et al.* reported the first case of an erionite-associated malignant mesothelioma in North America [15]. The individual in that report was raised in Villa Guerrero, Jalisco, Mexico,

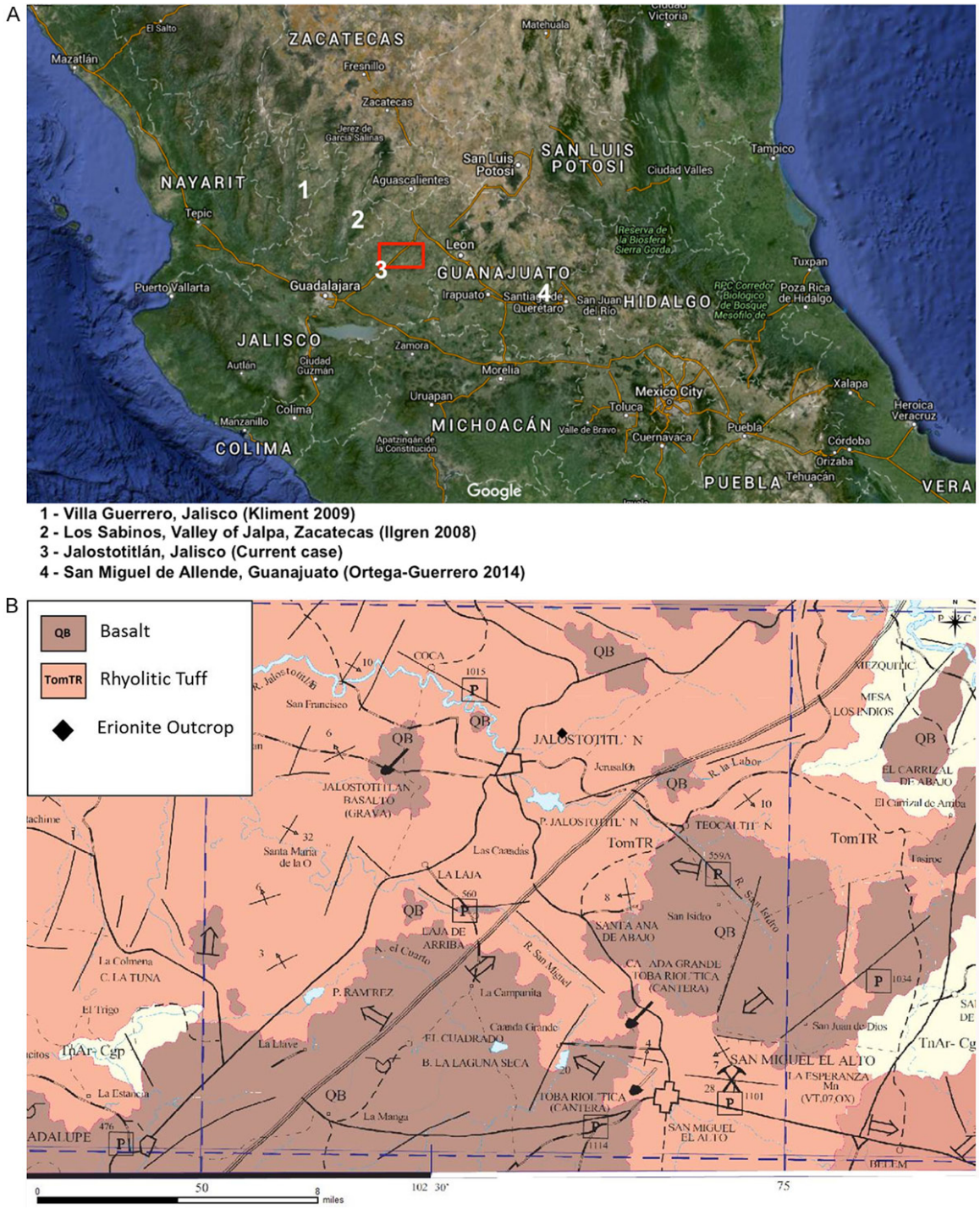

Figure 1. Summary of Mexican malignant mesothelioma reports. A. Map of the Mexican Volcanic Belt region showing the proximity of areas with known cases of erionite-associated mesothelioma (1, 3) or elevated mesothelioma rates (2, 4). Key: 1) Villa Guerrero, Jalisco [15]; 2) Los Sabinos, Valley of Jalpa, Zacatecas; [2] 3) Jalostotitlán, Jalisco (current case); 4) San Miguel de Allende, Guanajuato [14]. B. Geological map of specific region of interest, boxed in map 1A. Information obtained from reference [17].

suggesting that there may be a potential risk for environmental exposure to this mineral in this region (**Figure 1**). Furthermore, high amounts of airborne erionite were found in North Dakota after hundreds of miles of roads were surfaced with erionite-containing gravel [16].

Table 1. Summary of samples collected and analyzed from the patient's homestead in Jalostotilán, Mexico

Site	Description	PLM Results	XRD Results for Erionite (%)
1	Northern room adobe brick	No erionite detected	No erionite detected
1	Northern room white wash	No erionite detected	No erionite detected
1	Northern room mortar used between the adobe	No erionite detected	No erionite detected
1	Middle room white wash	No erionite detected	No erionite detected
1	Tuffaceous material used in wall, southern most room (granary)	No erionite detected	No erionite detected
1	Tuffaceous material used in wall, southern most room (granary)	No erionite detected	No erionite detected
1	White wash, southern most room	No erionite detected	No erionite detected
2	Tuff material, friable	Confirmed erionite n_{ω} < 1.480; + elongation	0.94
3	Tuff material, friable	Confirmed erionite n_{ω} < 1.480; + elongation	0.55
4	Soil material from cornfield	Confirmed erionite n_{ω} < 1.480; + elongation	< Detection Limit
4	Tuff underlying cornfield only 4-6 inches down	Confirmed erionite n_{ω} < 1.480; + elongation	< Detection Limit
5	Fine grained tuff material	No erionite detected	No erionite detected
5	Coarse grained tuff material	No erionite detected	No erionite detected
5	Coarse tuff with slight pink coloration	No erionite detected	No erionite detected
6	Standing water in a stream cutting through the tuff	N/A	N/A
7	Road cut	No erionite detected	No erionite detected
8	Picked out clasts of vitric materials	No erionite detected	No erionite detected
8	Tuff bulk sample	No erionite detected	No erionite detected
8	Tuff bulk sample	No erionite detected	No erionite detected
8	Vitreous clasts	No erionite detected	No erionite detected

PLM - polarized light microscopy. XRD: x-ray powder diffraction. Samples were collected from eight sites around the family homestead in Mexico: 1) the family home made of adobe brick, 2) an outcrop of rhyolitic tuff on a trail near the house, 3) a well on the property, 4) soil and tuff from the cornfields, 5) exposed rhyolitic tuff near a stream, 6) a standing pool of water at the stream, 7) a road that cut through the homestead, and 8) an active quarry near the farm. Erionite was found by PLM in samples from sites two, three, and four and levels were quantified by XRD for samples from sites two and three.

Erionite, therefore, may pose a significant public health risk in multiple regions of North America.

Here, we report a second case of erionite-associated epithelial malignant pleural mesothelioma in North America and identify the probable exposure source in soil from the farm in Mexico on which the patient was raised.

Materials and methods

Case history

This case involved a 53-year-old male with a diagnosis of epithelial malignant pleural mesothelioma. The patient was raised on his family's farm that was located just east of the city of Jalostotitlán, Jalisco, Mexico until he moved to the United States as a young adult. Jalostotitlán is in the Mexican Volcanic Belt and the surface geology specific to this area is described as rhyolitic tuff that was deposited during the late Oligocene through the early Miocene [17]. Other occurrences of erionite in similar aged rhyolitic tuffs have been documented farther east in the state of Guanajuato in central Mexico [18]. As a child, the patient actively helped on the farm, digging holes for fences, tilling land for the planting of beans and corn, and using water from the well. From 1980 through 2000, he worked as a vehicle repairman in California and may have worked with asbestos-containing friction materials. The man's father, a farmer in Mexico, died of a pleural mesothelioma (as per his death certificate) at the age of sixty-one and had no known history of asbestos exposure.

Gross pathology and histological lung tissue analysis

At the time of diagnosis, a left pleurectomy and decortication was performed on the patient along with a partial resection of the diaphragm. Tissue sections from the pleurectomy specimen were stained for various markers of mesothelioma and other cancers.

Lung digest and fiber analysis

Paraffin blocks containing pieces of the left lower lobe of the lung that was resected at the time of pleurectomy were deparaffinized in

xylene and rehydrated to 95% ethanol. The final wet weight of lung tissue not involved with tumor was 0.181 g. This tissue was digested using the sodium hypochlorite method as previously described [19]. For analysis, the residue was placed on a 0.4 micron pore size Nuclepore filter, and the filter was cut in two. One half of the filter was mounted on a glass slide for asbestos body quantification by light microscopy at 200× magnification. The other half was mounted on a carbon disc with colloidal graphite and sputter coated with platinum for fiber analysis by scanning electron microscopy (SEM) and energy dispersive x-ray analysis (EDXA).

Environmental fiber analysis

Rock, soil, and building material samples were collected from the patient's family homestead in Jalostotitlán, Jalisco, Mexico, about 100 km northeast of Guadalajara and 400 km northwest of Mexico City (21° 10' 45" N and 102° 26' 44" W) (**Figure 1**). Samples were gathered from eight sites around the homestead (summarized in **Table 1**): 1) the family home made of adobe brick, 2) an outcrop of rhyolitic tuff on a trail near the house, 3) a well on the property, 4) soil and tuff from the cornfields, 5) exposed rhyolitic tuff near a stream, 6) a standing pool of water at the stream, 7) a road that cut through the homestead, and 8) an active quarry near the farm.

The rock samples were first analyzed by polarized light microscopy (PLM). Each non-aqueous sample was ground in mortar and pestle and mounted on glass slides using a 1.480 refractive index liquid (erionite has a refractive index of $\alpha = 1.468$ and $\gamma = 1.480$ [20]).

To confirm the PLM results, bulk samples were also analyzed using x-ray powder diffraction (XRD). Using XRD, a unique erionite peak may be seen in the range of 7.6 - 7.8 °2θ with a detection limit of 0.1% (there must be more than 0.1 percent by weight to see a definitive peak in this range). Two scans were carried out for each sample: 1) a scan from 4 - 64 °2θ and 2) a scan from 6 - 12 °2θ. Quantification of erionite in samples from sites two and three was carried out by spiking in known concentrations of erionite from Rome, Oregon and creating a calibration curve as previously described [21].

Erionite fibers from sites two and three were examined using SEM and transmission electron microscopy (TEM). TEM was also carried out on water samples from site six that could not be examined using the above-described methods. TEM was performed at the University of Idaho on a JEOL JEM 2010 TEM using a double tilt stage, and EDXA was performed using a Thermo Scientific detector coupled with NSS software. Samples were run at an accelerating voltage of 200 kV. Sample preparation techniques were modeled after the Jaffe-Wick method [22]. Briefly, samples were crushed with an agate mortar and pestle, diluted, and sonicated before being placed onto a 0.2 µm PCE filter and dried thoroughly. The sample was then carbon coated, and a 5 mm by 5 mm square was cut and mounted on a copper TEM grid for analysis.

Results

Pathology and histology

Grossly, extensive nodular tumor was found to involve the patient's diaphragm, pericardium, and visceral pleura (**Figure 2A**). Histologic sections from the surgery showed an invasive epithelial tumor involving all of these components with invasion into the lung parenchyma (**Figure 2B**, **2C**). Tumor from left lung tissue stained positive for calretinin in the nucleus and cytoplasm (**Figure 2D**), positive for cytokeratin 5/6 (**Figure 2E**), and positive for D2-40 in a membranous distribution (not illustrated). The tumor also displayed patchy nuclear staining for Wilms tumor 1 (WT1) (**Figure 2F**). The tumor was negative for CD15, carcinoembryonic antigen (CEA), prostate-specific antigen (PSA), Ber-EP4, and B72.3. This staining pattern is consistent with that of an epithelial mesothelioma [1].

Lung fiber analysis

No asbestos bodies were identified upon examination of an entire half filter of digested lung residue by light microscopy. This finding is equivalent to fewer than 7.7 asbestos bodies per gram of wet lung tissue, which is within the normal range of 0-20 asbestos bodies per gram [19].

By SEM, no asbestos bodies were identified in 100 consecutive fields (1000× magnification). There were 53,700 uncoated fibers per gram of

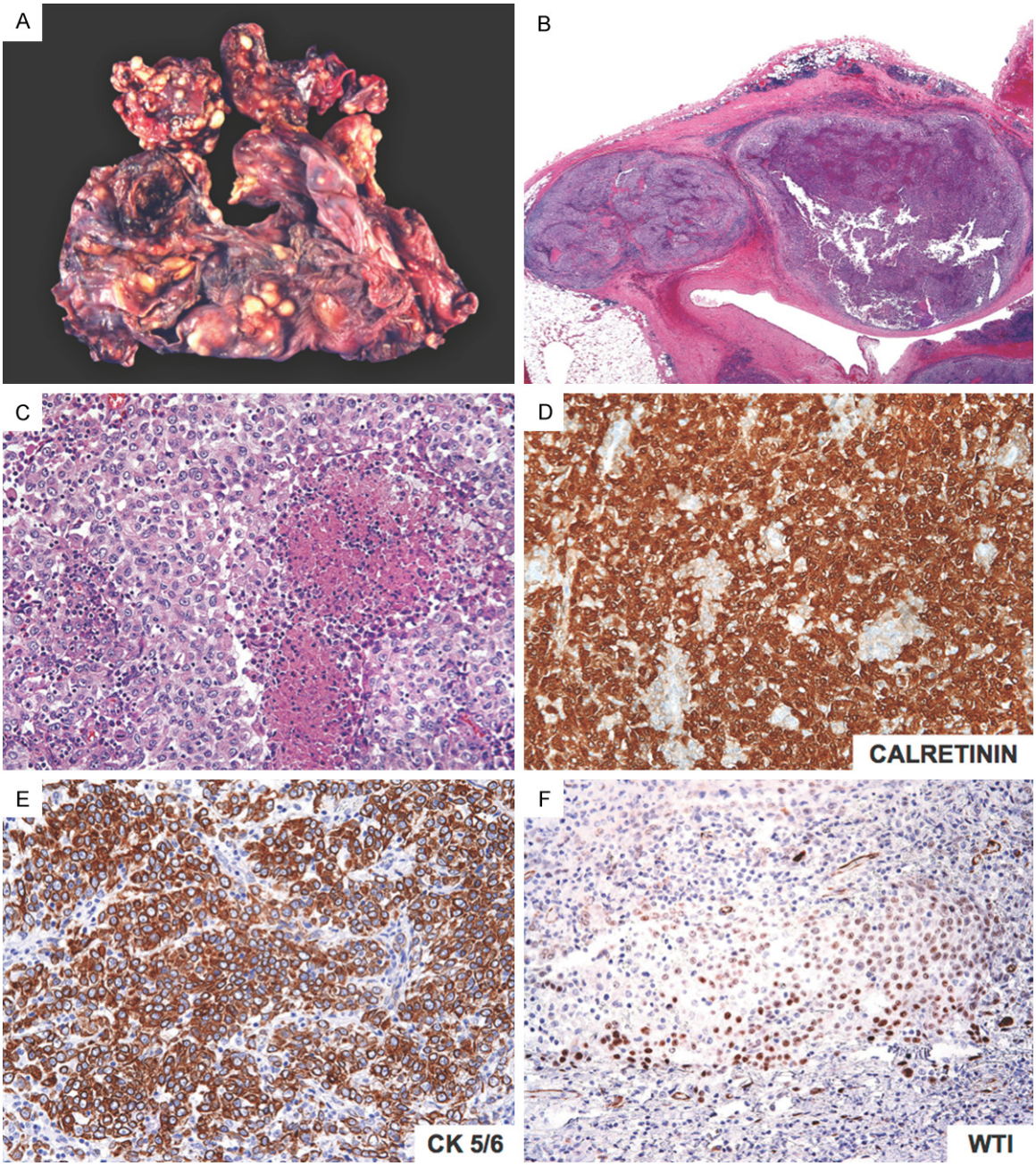

Figure 2. Gross pathology and histological analysis of tumor tissue shows malignant pleural epithelial mesothelioma. A. Pleurectomy specimen showing numerous neoplastic nodules ranging in size from 0.3 cm to 2.5 cm. B. Low power magnification of nodular lesions embedded within the parietal pleura (H&E 6.25×). C. High power magnification of epithelioid cells admixed with necrosis and scattered chronic inflammatory cells (H&E 200×). D. Calretinin stain highlighting the neoplastic cells (200×). E. Strong immunoreactivity against CK5/6 (200×). F. Patchy nuclear staining with WT1 stain (200×).

wet lung tissue. Twenty consecutive uncoated fibers were examined by EDXA, eighteen of which were aluminum silicates and two of which were sodium magnesium aluminum iron silicates (**Figure 3A** and **3B**). No asbestos fibers were found. The morphology and composition of the fibers are most consistent with erionite (fibrous zeolite).

Environmental fiber analysis

Fibrous erionite was detected in samples from sites two, three, and four (**Table 1**). These three locations were at elevations ranging from 1,768 to 1,771 meters above sea level. The other sampled tuffs were at lower elevations and were found to contain no evidence of zeolite

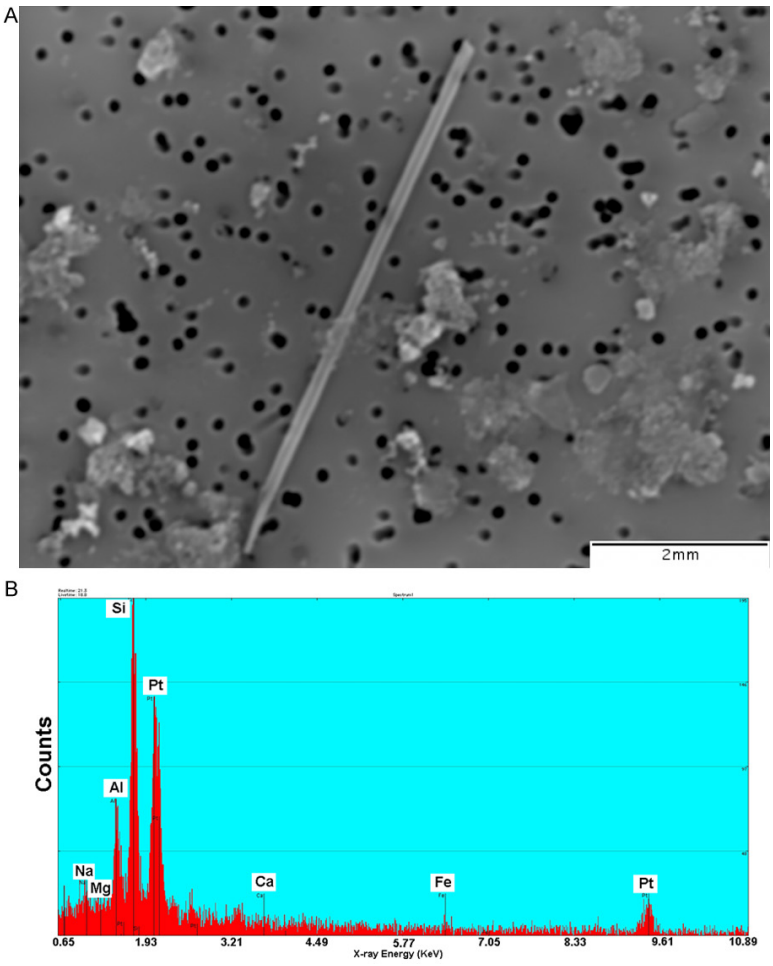

Figure 3. Lung digestion fiber analysis reveals fibrous erionite in patient's lung tissue. A. Secondary electron image of erionite fiber recovered from the patient's lung tissue. The pores on the Nuclepore filter in the background have a diameter of 0.4 μm. Magnified 4000×. B. Energy dispersive spectrum from erionite fiber, showing peaks for aluminum and silicon. There is a suggestion of smaller peaks for sodium and iron. Platinum peaks are from sputter-coating the sample for imaging purposes.

formation. Sites two and three had the highest concentration of fibers. These fibers were the ones that could be observed by both PLM (**Figure 4A** and **4B**) and XRD (**Figure 4C**). After calibration was performed with erionite from Rome, Oregon, the samples from sites two and three were found to contain 0.9 percent and 0.5 percent erionite, respectively by quantitative powder XRD. Though fibers from site four were observed using PLM, they were below the detection limit for XRD.

SEM analysis of *in situ* erionite from samples from sites two and three illustrates that erionite fibers form primarily in cavities from the rhyolitic tuff (**Figure 5A** and **5B**). The rhyolitic tuff from sites two, three, and four was found to be friable. TEM analysis revealed fibers that were 1 μm or thinner and had lengths from 5 - 20 μm. (**Figure 6A**) The identity of the fibers as erionite was confirmed with the selected area electron diffraction (SAED) patterns of representative fibers (**Figure 6B**).

Discussion

This report describes a case of erionite-associated malignant pleural epithelial mesothelioma, proven by lung digestion studies and fiber composition analysis. A detailed analysis of the environmental exposure source is also presented: rock, soil, and building material samples from the patient's childhood family farm that reveal erionite deposits in the soil.

This case first came to our attention as a medical-legal consultation that was seeking to determine if there was any evidence of occupational asbestos exposure in the patient. The patient was reported to have worked around asbestos-containing friction materials for many years as a repairman, yet epidemiological studies have shown no increased rates of mesotheliomas in mechanics [23-28]. However, other investigations have shown that carrying out lung digestion studies in these cases can uncover other likely causes of mesothelioma. For example, in one study, half of the lung digestion studies from workers exposed to friction products showed elevated levels of commercial amphiboles in their lung tissue [29]. As friction products do not contain commercial amphiboles, these findings indicate that these individuals were exposed to asbestos from another product or source. Here we demonstrate the discovery of erionite fibers as a likely cause of this patient's malignant mesothelioma since no asbestos fibers in excess of background were found in this patient's lung.

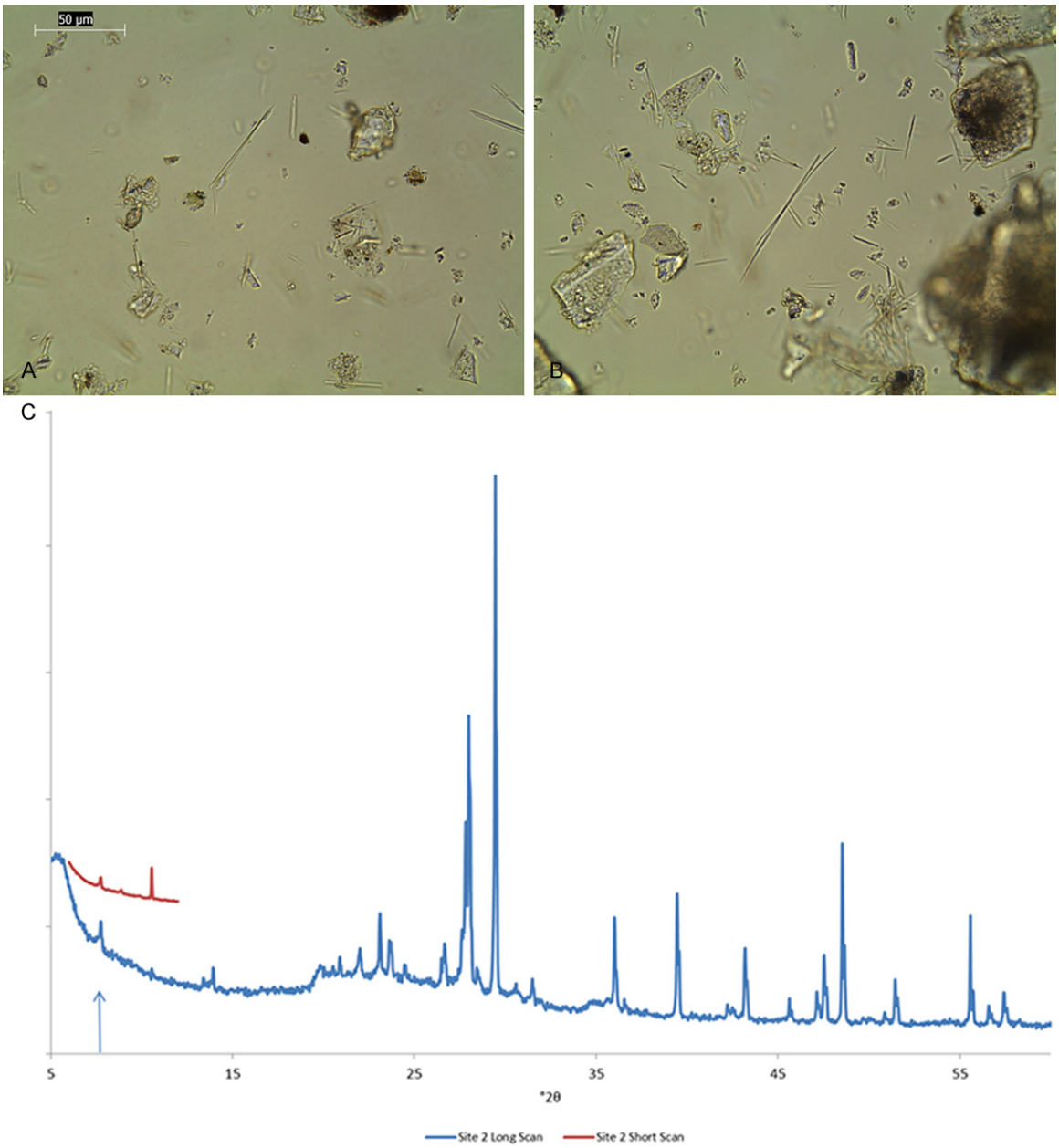

Figure 4. Polarized light microscopy (PLM) and x-ray powder diffraction (XRD) of soil samples from Mexico (sites two and three) show presence of zeolite. (A) PLM image of friable tuff material in plane polarized light from site two and (B) site three. (C) Long (blue) and short (red) XRD scan of friable tuff material from site two. The arrow points to the location of the primary zeolite peak.

It is important to note that when attributing causation of a mesothelioma to prior asbestos exposure, the most often cited criteria are the "Helsinki Criteria" [30]. The Helsinki Criteria for asbestos-related disease diagnosis highlight the importance of pathological studies such as lung fiber counts, autopsy findings, and histological tissue analysis to identify mesotheliomas caused by asbestos exposure [30]. However, the criteria also state that, "In the absence of such markers, a history of significant occupational, domestic, or environmental exposure to asbestos will suffice for attribution". This is often misconstrued to mean that without pathological evidence of asbestos-associated disease (that is, the studies were carried out and no asbestos-associated pathology was seen), any exposure history to asbes-

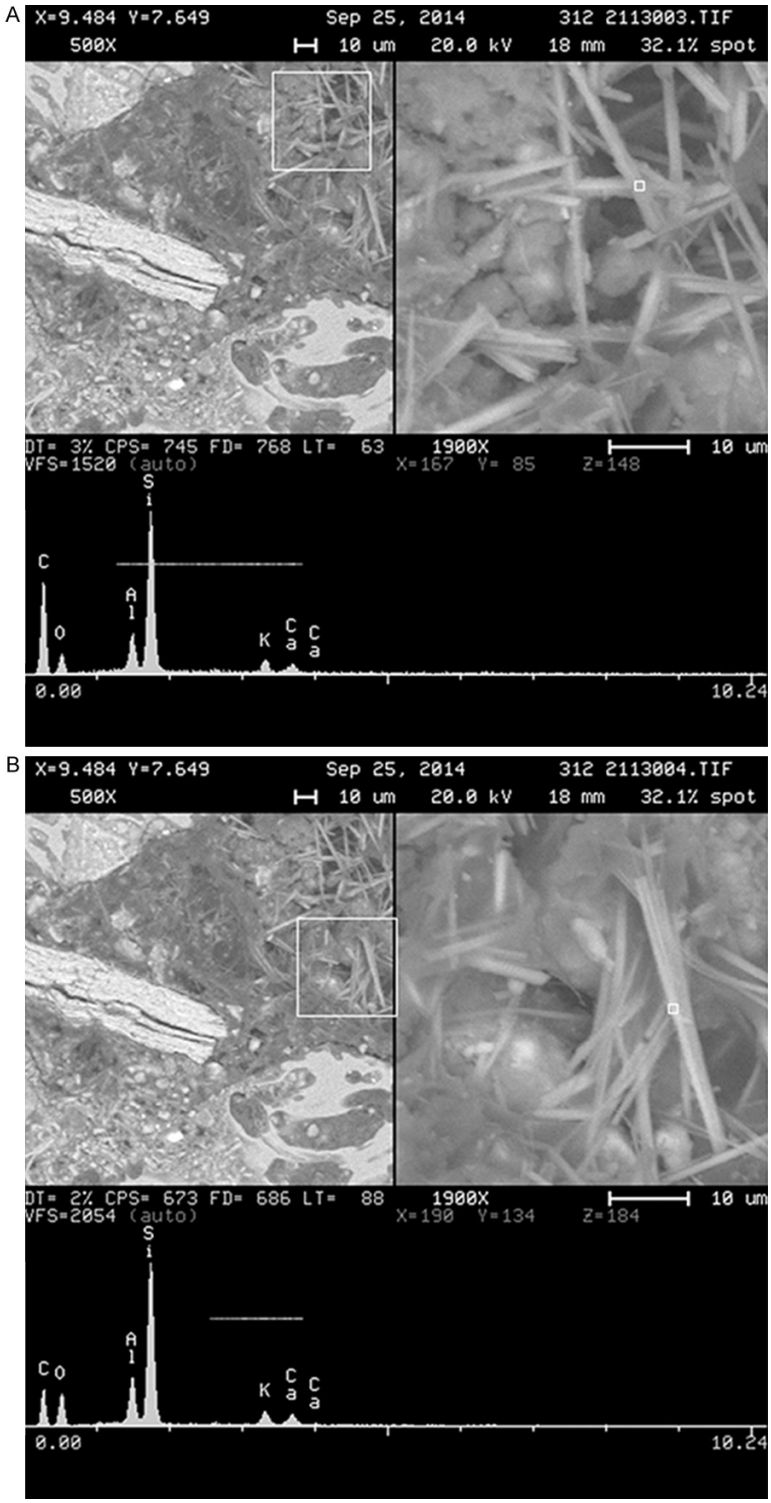

Figure 5. Scanning electron microscopy images of erionite in soil samples from Mexico. (A and B) are two SEM images of the site two friable tuff material that was analyzed in **Figure 4**.

tos, no matter how small, is sufficient to link the mesothelioma to asbestos. As this case demonstrates, this is not always accurate. As such, this case highlights the importance of lung tissue fiber analysis. Tissue digestion studies are the most objective and accurate way to identify the causative agent in cases of mesothelioma and should be the primary method for determining causation in these cases when lung tissue is available. Because mesothelioma has a poor prognosis and most patients unfortunately die from their cancer, identifying the causative agent does not play an important role in terms of diagnosis and treatment. However, since many of these cases involve posthumous legal action, lung autopsy samples may be collected and saved for the more objective digestion studies and definitive diagnosis. This could have important implications not only for legal disputes, but also for the health of surviving family members and the larger community. This patient's father also died of pleural mesothelioma (as noted on his death certificate), raising the possibility that both the father and son's mesotheliomas were due to erionite exposure at the family farm. This region of Mexico has also been found to have elevated rates of mesothelioma with no obvious asbestos industry [2, 14]. Thus, digestion studies can be useful to determine potential risks of exposure so that further actions can be taken to reduce the risks to others.

Erionite is found in a widespread region of North America and it has been postulated that the United States may have the largest deposits of erionite in the world [31]. Therefore,

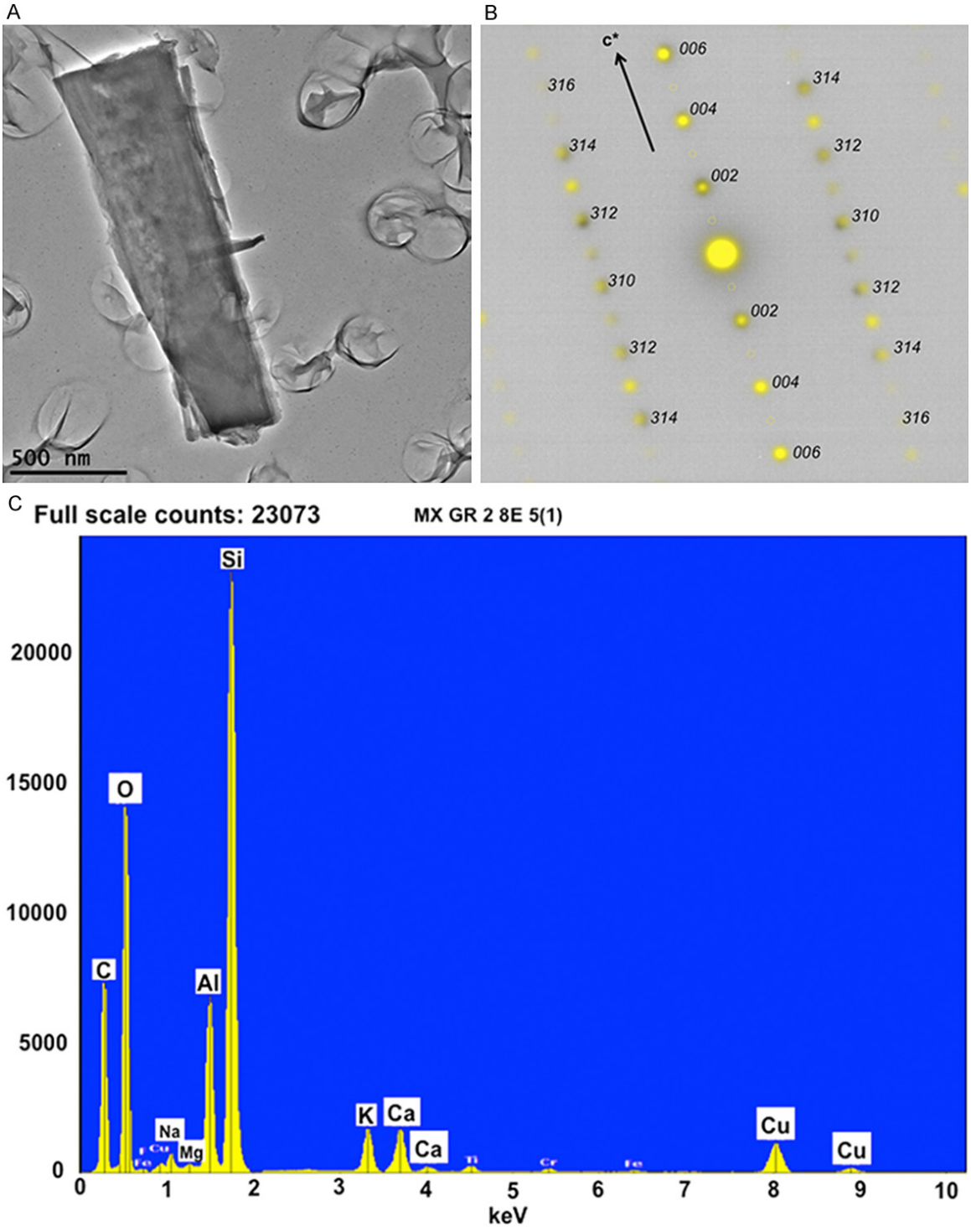

Figure 6. Transmission electron microscopy analysis of Mexican soil samples confirms identity of erionite fibers in the soil. A. TEM SAED image of Mexican erionite (scale = 500 nm). B. Indexed diffraction pattern taken along the 130-zone axis. Yellow dots indicate indexed pattern. Black dots indicate actual diffraction pattern. C. EDXA highlighting major elemental composition of the Mexican soil erionite.

as the population expands into more rural areas of the west and Rocky Mountain region, care should be taken to limit disturbance of erionite fibers from the soil. Healthcare profes-

sionals should also be aware of the increased risk of erionite-associated mesotheliomas in people from these regions so that appropriate studies can be done on individuals that develop mesotheliomas in these areas to determine if erionite exposures are contributing to the pathogenesis of this disease.

Acknowledgements

E.A.O. was supported by the National Institute of Environmental Health Sciences Ruth L. Kirschstein National Research Service Award 1F30ES024045.

Disclosure of conflict of interest

T.D.O. and V.L.R. are medical-legal consultants for asbestos-related litigation. M.S.S. and D.R.V.O. do fiber analysis and serve as expert witnesses in asbestos litigation cases. M.E.G. serves as an expert witness in issues dealing with characterization of natural materials. All other authors declare no conflicts of interest.

Abbreviations

EDXA, energy dispersive x-ray analysis; PLM, polarized light microscopy; SAED, selected area electron diffraction; SEM, scanning electron microscopy; TEM, transmission electron microscopy; XRD, x-ray powder diffraction.

Address correspondence to: Dr. Tim D Oury, Department of Pathology, University of Pittsburgh School of Medicine, S785 Scaife Hall, 3550 Terrace St., Pittsburgh, PA 15261, USA. Fax: 1-412-648-9527; E-mail: tdoury@pitt.edu; eao14@pitt.edu

References

[1] Pavlisko EN and Sporn TA. Mesothelioma. In: Oury TD, Sporn TA, Roggli VL, editors. Pathology of Asbestos-Associated Diseases. 3rd. New York: Springer; 2014. pp. 81-140.

[2] Ilgren EB, Ortega Breña M, Castro Larragoitia J, Loustaunau Navarrete G, Fuentes Breña A, Krauss E and Fehér G. A Reconnaissance Study of a Potential Emerging Mexican Mesothelioma Epidemic due to Fibrous Zeolite Exposure. Indoor and Built Environment 2008; 17: 496-515.

[3] Ortega-Guerrero MA and Carrasco-Nunez G. Environmental occurrence, origin, physical and geochemical properties, and carcinogenic potential of erionite near San Miguel de Allende, Mexico. Environ Geochem Health 2014; 36: 517-529.

[4] Maltoni C, Minardi F and Morisi L. Pleural mesotheliomas in Sprague-Dawley rats by erionite: first experimental evidence. Environ Res 1982; 29: 238-244.

[5] Hill RJ, Edwards RE and Carthew P. Early changes in the pleural mesothelium following intrapleural inoculation of the mineral fibre erionite and the subsequent development of mesotheliomas. J Exp Pathol (Oxford) 1990; 71: 105-118.

[6] Baris YI, Sahin AA, Ozesmi M, Kerse I, Ozen E, Kolacan B, Altinors M and Goktepeli A. An outbreak of pleural mesothelioma and chronic fibrosing pleurisy in the village of Karain/Urgup in Anatolia. Thorax 1978; 33: 181-192.

[7] Artvinli M and Baris YI. Malignant mesotheliomas in a small village in the Anatolian region of Turkey: an epidemiologic study. J Natl Cancer Inst 1979; 63: 17-22.

[8] Sebastien P, Gaudichet A, Bignon J and Baris YI. Zeolite bodies in human lungs from Turkey. Lab Invest 1981; 44: 420-425.

[9] Aguilar-Madrid G, Robles-Perez E, Juarez-Perez CA, Alvarado-Cabrero I, Rico-Mendez FG and Javier KG. Case-control study of pleural mesothelioma in workers with social security in Mexico. Am J Ind Med 2010; 53: 241-251.

[10] McDonald AD and McDonald JC. Malignant mesothelioma in North America. Cancer 1980; 46: 1650-1656.

[11] Enterline PE. Cancer produced by nonoccupational asbestos exposure in the United States. J Air Pollut Control Assoc 1983; 33: 318-322.

[12] Enterline PE and Henderson VL. Geographic patterns for pleural mesothelioma deaths in the United States, 1968-81. J Natl Cancer Inst 1987; 79: 31-37.

[13] Connelly RR, Spirtas R, Myers MH, Percy CL and Fraumeni JF Jr. Demographic patterns for mesothelioma in the United States. J Natl Cancer Inst 1987; 78: 1053-1060.

[14] Ortega-Guerrero MA, Carrasco-Nunez G, Barragan-Campos H and Ortega MR. High incidence of lung cancer and malignant mesothelioma linked to erionite fibre exposure in a rural community in Central Mexico. Occup Environ Med 2015; 72: 216-218.

[15] Kliment CR, Clemens K and Oury TD. North american erionite-associated mesothelioma with pleural plaques and pulmonary fibrosis: a case report. Int J Clin Exp Pathol 2009; 2: 407-410.

[16] Carbone M, Baris YI, Bertino P, Brass B, Comertpay S, Dogan AU, Gaudino G, Jube S, Kanodia S, Partridge CR, Pass HI, Rivera ZS, Steele I, Tuncer M, Way S, Yang H and Miller A. Erionite exposure in North Dakota and Turkish

villages with mesothelioma. Proc Natl Acad Sci U S A 2011; 108: 13618-13623.
[17] Carta Geologico-Minera Aguascalientes F13-9. El Servicio Geologico Mexicano, 1998.
[18] dePabloGalan L and ChavezGarcia MD. Diagenesis of oligocene vitric tuffs to zeolites, Mexican volcanic belt. Clays and Clay Minerals 1996; 44: 324-338.
[19] Roggli VL and Sharma A. Analysis of tissue mineral fiber content. In: Oury TD, Sporn TA, Roggli VL, editors. Pathology of Asbestos-Associated Diseases. 3rd. New York: Springer; 2014. pp. 253-292.
[20] Fleischer M, Wilcox RE, Matzko JJ and Geological Survey (U.S.). Microscopic determination of the nonopaque minerals. Washington, D.C.: U.S. Dept. of the Interior For sale by the Supt. of Docs., U.S. G.P.O., 1984.
[21] Bish DL and Chipera SJ. Detection of Trace Amounts of Erionite Using X-Ray-Powder Diffraction - Erionite in Tuffs of Yucca Mountain, Nevada, and Central Turkey. Clays and Clay Minerals 1991; 39: 437-445.
[22] Yamate G, Agarwal SC and Gibbons RD. Methodology for the measurement of airborne asbestos by electron microscopy, Environmental Monitoring Systems Library, Office of Research and Development, U.S. Environmental Protection Agency, 1984.
[23] Goodman M, Teta MJ, Hessel PA, Garabrant DH, Craven VA, Scrafford CG and Kelsh MA. Mesothelioma and lung cancer among motor vehicle mechanics: a meta-analysis. Ann Occup Hyg 2004; 48: 309-326.
[24] Laden F, Stampfer MJ and Walker AM. Lung cancer and mesothelioma among male automobile mechanics: a review. Rev Environ Health 2004; 19: 39-61.
[25] Hessel PA, Teta MJ, Goodman M and Lau E. Mesothelioma among brake mechanics: an expanded analysis of a case-control study. Risk Anal 2004; 24: 547-552.
[26] Rake C, Gilham C, Hatch J, Darnton A, Hodgson J and Peto J. Occupational, domestic and environmental mesothelioma risks in the British population: a case-control study. Br J Cancer 2009; 100: 1175-1183.
[27] Garabrant DH, Alexander DD, Miller PE, Fryzek JP, Boffetta P, Teta MJ, Hessel PA, Craven VA, Kelsh MA and Goodman M. Mesothelioma among Motor Vehicle Mechanics: An Updated Review and Meta-analysis. Ann Occup Hyg 2016; 60: 8-26.
[28] Marsh GM, Youk AO and Roggli VL. Asbestos fiber concentrations in the lungs of brake repair workers: commercial amphiboles levels are predictive of chrysotile levels. Inhal Toxicol 2011; 23: 681-688.
[29] Butnor KJ, Sporn TA and Roggli VL. Exposure to brake dust and malignant mesothelioma: a study of 10 cases with mineral fiber analyses. Ann Occup Hyg 2003; 47: 325-330.
[30] Asbestos, asbestosis, and cancer: the Helsinki criteria for diagnosis and attribution. Scand J Work Environ Health 1997; 23: 311-316.
[31] Brobst DA and Pratt WP. United States mineral resources. Washington: United States Govt. Printing Off; 1973.